Korean J. Chem. Eng., **17**(6), 659-667 (2000)

Hydrate Phase Equilibria for Gas Mixtures Containing Carbon Dioxide: A Proof-of-Concept to Carbon Dioxide Recovery from Multicomponent Gas Stream

Yu-Taek Seo, Seong-Pil Kang, Huen Lee†, Chul-Soo Lee* and Won-Mo Sung**

Department of Chemical Engineering, Korea Advanced Institute of Science and Technology, 393-1, Kusong-dong, Yusong-gu, Taejon, Korea
*Department of Chemical Engineering, Korea University, Seoul 136-701, Korea
**Section of Geosystem and Environmental Engineering, Hanyang University, Seoul 133-791, Korea
(*Received 18 May 2000 • accepted 14 July 2000*)

Abstract−Three-phase equilibrium conditions (aqueous liquid-hydrate-vapor) of CO_2-N_2 binary mixtures in the temperature range of 271.75 K to 284.25 K and the pressure range of 12 to 235 bar. In addition, three-phase (aqueous liquid-hydrate-vapor) behavior for CO_2-CH_4 mixture were measured in the temperature range of 272 to 284 K at the constant pressures of 15, 20, 26, 35 and 50 bar. In high concentration of CO_2, upper quadruple points were also measured. The obtained data indicates that three-phase equilibrium temperatures become higher with increasing concentration of CO_2. For the prediction of three-phase equilibrium, the vapor and liquid phases were treated by employing the Soave-Redlich-Kwong equation of state (SRK-EOS) with the second order modified Huron-Vidal (MHV2) mixing rule and the hydrate phase with the van der Waals-Platteeuw model. The calculated results showed good agreement with experimental data. The concentration of vapor and hydrate phases was also determined experimentally. This work can be used as the basic data for selective separation process by hydrate formation.

Key words: Hydrate, Phase Equilibria, Carbon Dioxide, Methane, Thermodynamics

INTRODUCTION

Gas hydrates are crystalline compounds that are formed by physically stable interaction between water and relatively small guest molecules occupied in the cavities built by water molecules. The hydrates of the various gases may have structures corresponding to the fundamental types S_I or S_{II}. Mixtures containing more than one gas constituent can similarly form a hydrate structure of one kind, but it is possible that the hydrates of the individual constituents are characterized by different structures.

Predictions of global energy use in the next century suggest a continued increase in emissions and rising concentrations of CO_2 in the atmosphere unless we manage fossil fuel energy use. One way to manage CO_2 is to use energy resources more efficiently to reduce our energy demand. Another way is to increase the low-carbon and carbon-free fuels and technologies such as nuclear power, solar energy, wind power, and biomass fuels. The third and newest way is to manage carbon, capturing or separating and securely storing CO_2 freely vented from the energy system. There are numerous methods for the separation and capture of CO_2, and many of these are commercially available: for example, cryogenic fractionation, selective adsorption, gas absorption, and the like. Although these processes have proved successful for the selective removal of CO_2 from multi-component gaseous stream, they are energy intensive. Accordingly, there is continuing interest in the development of a less energy intensive process for the selective separation of CO_2 from multi-component gaseous streams. Hydrate formation method is less energy intensive and has a huge potential capability of separating CO_2. In addition to such separation processes, CO_2 plays a substantial industrial role in gas production and processing. In the earth's permafrost and ocean floors, there are large resource deposits of CO_2 and hydrocarbon hydrates. Makogon in 1997 estimated that the concentration of carbon dioxide in hydrate deposits is usually 0.1 to 4.6 mole percent. Since CO_2 is normally produced with hydrocarbons, hydrate equilibrium conditions of binary gas mixture containing CO_2 are good information for checking the possibility of CO_2 separation.

If a system containing only one type of hydrate is formed, the phenomenon corresponding to complete mixing of the solid solution is manifested, and thus a mixed hydrate is formed. Until now there are several studies about hydrate equilibrium conditions of various binary gas mixture systems. Unruh and Katz [1949] reported the phase equilibrium data for the CH_4-CO_2-H_2O system and determined vapor phase concentration indirectly. Berecz and Balla-Achs [1983] showed that hydrates of CH_4 and CO_2 mixture exhibited instability at CO_2 mole fraction of 50 mol% and higher. Adisasmito et al. [1991] confirmed and extended the Unruh and Katz data. They showed that the result of Berecz and Balla-Achs was very unusual, and the equilibrium conditions in isobaric conditions were not investigated precisely. But, their work showed that appropriate selection of the optimum pressure conditions could suggest the separation method of CO_2 content from CH_4-rich gases. If

†To whom correspondence should be addressed.
E-mail: hlee@hanbit.kaist.ac.kr
This paper was presented at The 5th International Symposium on Separation Technology-Korea and Japan held at Seoul between August 19 and 21, 1999.

two binary systems form hydrates of different types, then partial mixing of the solid solutions can be detected in the ternary system. In the CH_4-C_3H_8-H_2O system, the gas constituents form hydrate with different structures. van der Waals and Platteeuw [1959] gave a detailed evaluation of the composition of the hydrate formed at 270.15 K. At the composition range below about 0.5 mol% of C_3H_8 the system showed complicated phase behavior. Thakore and Holder [1987] reported the equilibrium conditions of the same system over the ice point, that is, 275.15 K and 278.15 K. Similar to CH_4-C_3H_8 hydrate, C_3H_8-H_2S hydrate system was also investigated in detail by van der Waals and Platteeuw [1959] at a temperature of 270.15 K. They found that the hydrate formed was not a stoichiometric double hydrate, but a mixed hydrate with varying composition. Although the resulting hydrate structure resembled that of CH_4-C_3H_8 hydrate, an azeotropic system was formed. Jhaveri and Robinson [1965] reported the equilibrium conditions of the CH_4-N_2 hydrate. The composition of the equilibrium vapor and hydrate phase was determined experimentally by gas chromatography at 273.15 and 279.82 K. The information would be of value in determining the hydrate-forming conditions in CH_4-rich natural gases containing N_2.

In this study, the isobaric equilibrium conditions of CO_2 and CH_4 mixture were measured to identify the hydrate-forming region, and the equilibrium conditions of CO_2 and N_2 mixture were also measured. The measured hydrate equilibrium data were correlated by Soave-Redlich-Kwong equation of state (SRK-EOS) incorporated with the second order modified Huron-Vidal (MHV2) mixing rule and modified UNIFAC.

THERMODYNAMIC MODELING

Thermodynamic models for the calculation of hydrate equilibria have been derived and modified by several workers. A large number of relative studies have been discussed and reviewed in the literature [Berecz and Balla-Achs, 1983; Holder et al., 1988; Sloan, 1990; Englezos, 1993]. van der Waals and Platteeuw [1959] originally proposed a statistical thermodynamic model based on classical adsorption theory, that is, the Langmuir isotherm, and calculated the phase behavior of several binary and ternary hydrate-forming systems. According to the van der Waals and Platteeuw model, the fugacity of guest components in the vapor phase is in equilibrium with that in the hydrate phase. Therefore, the equilibrium relation of guest components between the hydrate and vapor phases is automatically satisfied. Then, the final equilibrium conditions for the hydrate forming system are determined by comparing the equality between the fugacity of water in the hydrate phase and that in any other phase. The Soave-Redlich-Kwong equation of state incorporated with a modified version of the Huron-Vidal mixing rule was used to determine the corresponding fugacity. Any appropriate excess Gibbs energy model for VLE calculations can be used for the Huron-Vidal mixing rules. In the present study, we use the modified UNIFAC model as the excess Gibbs energy model. All the UNIFAC parameters used in this study were cited from the literature. The thermodynamic model for hydrate phase was developed by van der Waals and Platteeuw, which related the chemical potential of water in the hydrate phase to that in hypothetical empty hydrate lattice. The fugacity of water in the hydrate phase is given

$$\hat{f}_w^H = f_w^{MT} \exp\left(-\frac{\Delta\mu_w^{MT-H}}{RT}\right) \tag{1}$$

where

$$-\frac{\Delta\mu_w^{MT-H}}{RT} = \sum_{m=1}^{k} \nu_m \ln\left(1 + \sum_{j=1}^{N_c} C_{mj} \hat{f}_j\right) \tag{2}$$

In the above equation, f_w^{MT} represents the fugacities of water in the hypothetical empty hydrate lattice, C_{mj} are the Langmuir constants. ν_m are the number of cavities of type m per water molecule in the hydrate lattice, N_c is the number of guest species, k is the number of cavity type in the hydrate lattice, and f_j are the fugacities of guest components in the vapor phase which are calculated by the equation of state. The quantity $\Delta\mu_w^{MT-H}$ ($=\mu_w^{MT}-\mu_w^H$) is the chemical potential difference between the empty hydrate and the filled hydrate phase.

The fugacity of water in the empty hydrate lattice, f_w^{MT}, is expressed differently depending on the temperature. If the temperature is below the ice point, 273.15 K,

$$f_w^{MT} = f_w^I \exp\left(\frac{\Delta\mu_w^{MT-I}}{RT}\right) \tag{3}$$

and if the temperature is above the ice point,

$$f_w^{MT} = f_w^L \exp\left(\frac{\Delta\mu_w^{MT-L}}{RT}\right) \tag{4}$$

where $\Delta\mu_w^{MT-I}=\mu_w^{MT}-\mu_w^I$ and $\Delta\mu_w^{MT-L}=\mu_w^{MT}-\mu_w^L$, respectively. The chemical potential differences can be calculated from an equation given by Holder et al. [1980]:

$$\frac{\Delta\mu_w^{MT-I}}{RT} = \frac{\Delta\mu_w^o}{RT} - \int_{T^o}^{T} \frac{\Delta h_w^{MT-I}}{RT^2} dT + \int_0^P \frac{\Delta v_w^{MT-I}}{RT} dP \tag{5}$$

$$\frac{\Delta\mu_w^{MT-L}}{RT} = \frac{\Delta\mu_w^o}{RT} - \int_{T^o}^{T} \frac{\Delta h_w^{MT-L}}{RT^2} dT + \int_0^P \frac{\Delta v_w^{MT-L}}{RT} dP - \ln a_w^* \tag{6}$$

$\Delta\mu_w^o$ is an experimentally determined quantity which denotes the difference between the chemical potential of the empty hydrate lattice and the pure host component at a reference temperature of T^o and zero absolute pressure. Similarly, Δh_w^{MT-L} and Δv^o denote the differences in enthalpy and volume, respectively. Also, a_w represents the activity of water calculated from an equation of state. A correlation for the enthalpy difference was also given by Holder et al. [1980].

Table 1. Reference parameters for gas hydrate of structure I and II

Reference parameter	Unit	Structure I	Structure II
$\Delta\mu_w^{o\dagger}$	J/mol	1,263.60	883.82
Δh_w^o	J/mol	1,389.08	1,025.08
Δv_ω^o	cm^3/mol	3.0	3.4
$\Delta C_{pw}^{MT-I\ddagger}$	J/mol · K	38.12-0.141(T-273.15)	

† : Values for S_I and S_{II} are from CSMHYD [Sloan, 1990].

‡ : Parrish and Prausnitz [1972].

*$\Delta h_w^{MT-L}=\Delta h_w^{MT-I}+\Delta h_w^{fus}$ and $\Delta v_w^{MT-L}=\Delta v_w^{MT-I}+\Delta v_w^{fus}$

$$\Delta h_w^{MT-L} = \Delta h_w^o + \int_{T^o}^{T} \Delta C_{pw}^{MT-I} dT \quad (7)$$

Several values for the reference parameters have been reported in the literature. In this work, the values reported by Parrish and Prausnitz [1972] and Sloan [1990] were used, and their values are given in Table 1.

Finally, the fugacity of water in the filled hydrate lattice is computed by the following two expressions:

$$\hat{f}_w^H = f_w^I \exp\left(\frac{\Delta\mu_w^{MT-I}}{RT} - \frac{\Delta\mu_w^{MT-H}}{RT}\right) \quad (8)$$

or

$$\hat{f}_w^H = f_w^L \exp\left(\frac{\Delta\mu_w^{MT-L}}{RT} - \frac{\Delta\mu_w^{MT-H}}{RT}\right) \quad (9)$$

depending on the system temperature.

The Langmuir constant considers the interaction between the guest-water molecules in the hydrate cavities, and the cavity potential function uses the Kihara potential with spherical core assumption, which is reported to give better results than the usual Lennard-Jones potentials for calculating the hydrate dissociation pressures [McKoy and Sinanoglu, 1963]. The Langmuir constant is given by

$$C_{m_j} = \frac{4\pi}{kT}\int_0^{R-a} \exp\left[-\frac{w(r)}{kT}\right] r^2 dr \quad (10)$$

where T is the absolute temperature, k is Boltzmann's constant, w(r) is the spherically symmetrical potential, and r is the radial distance from the center of the cavity.

The Kihara spherical core pair potential energy $\Gamma(x)$ between the guest molecule and any one of the host molecules comprising the cavity is related to the force F, which each exerts on the other by $F = \partial\Gamma(x)/\partial x$, where x is molecular center separation distance between the two. This potential is thus unique to every molecular type and is given as a function of separation distance by

$$\Gamma(x) = \infty;\ x \le 2a \quad (11)$$

$$\Gamma(x) = 4\varepsilon\left[\left(\frac{\sigma}{x-2a}\right)^{12} - \left(\frac{\sigma}{x-2a}\right)^{6}\right];\ x > 2a \quad (12)$$

where a is the radius of the spherical core, σ is the distance between the cores at zero potential energy and ε is the depth of the intermolecular potential well.

McKoy and Sinanoglu [1963] summed up all the Kihara spherical core pair interactions between the guest molecule and any one of the host molecules inside the cell. An overall cell potential w(r) can be represented as

$$w(r) = 2z\varepsilon\left[\frac{\sigma^{12}}{R^{11}r}\left(\delta^{10} + \frac{a}{R}\delta^{11}\right) - \frac{\sigma^{6}}{R^{5}r}\left(\delta^{4} + \frac{a}{R}\delta^{5}\right)\right] \quad (13)$$

where

$$\delta^N = \frac{1}{N}\left[\left(1 - \frac{r}{R} - \frac{a}{R}\right)^{-N} - \left(1 + \frac{r}{R} - \frac{a}{R}\right)^{-N}\right] \quad (14)$$

where N is equal to 4, 5, 10, or 11; z is the coordination number of the cavity, that is, the number of oxygen at the periphery of each

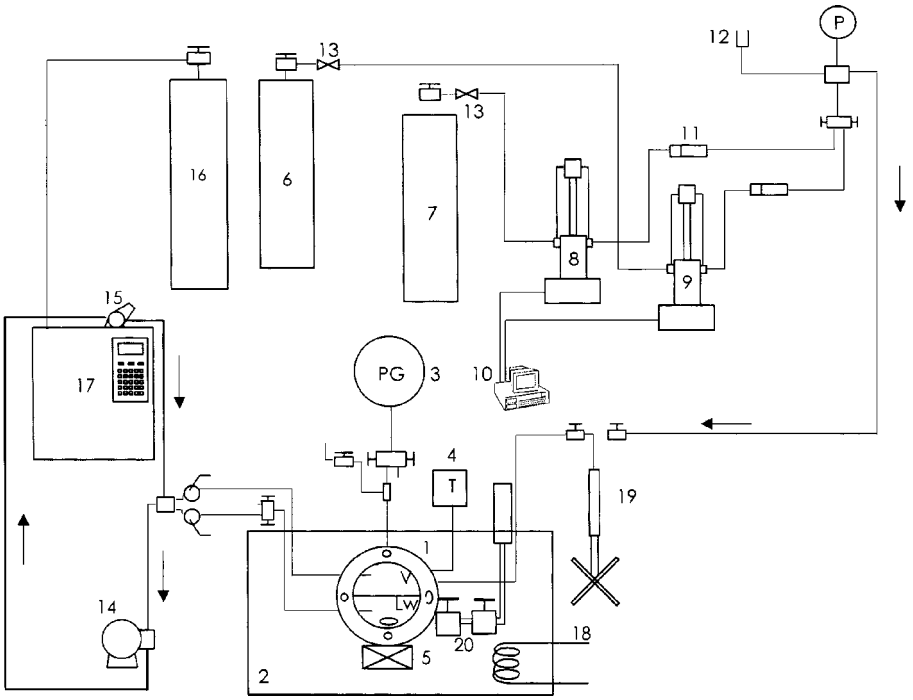

Fig. 1. Schematic diagram of the experimental apparatus used in this work.

1. Equilibrium cell
2. Water bath
3. Pressure gauge
4. Thermocouple
5. Magnetic stirrer
6. CO_2 cylinder
7. CH_4 cylinder
8, 9. Syringe pump
10. Multi controller
11. Check valve
12. Rupture disc
13. Line filter
14. High pressure pump
15. Sampling valve
16. Helium gas
17. Gas chromatograph
18. External heat exchanger
19. High pressure pump
20. Sampling port

cavity and these have been uniquely determined for each cavity type by X-ray diffraction data, and R is the radius of the cavity. The Kihara hard-core parameter, a, is given in the literature [Parrish and Prausnitz, 1972], while Kihara energy and size parameter, ε and σ, are obtained by fitting the model to the equilibrium data of the hydrate-forming system.

EXPERIMENTS

The CH_4 was supplied by the Scientific Gas Products Co. and had a purity of 99.99 mol%. World Gas Co supplied the CO_2 with a minimum purity of 99.9 mol%. The water was supplied from Sigma-Aldrich Chemical Co. with a purity of 99.1 mol%. N_2 with a minimum purity of 99.999 mol% was also purchased from the same company. Gas mixture of CO_2 and N_2 with specific concentration was not just prepared via gas chromatograph but also purchased from Duk Yang Gas Co., Korea. All chemicals were used without further purification. Doubly de-ionized water made in this laboratory was used.

A schematic diagram of the experimental apparatus used in this work is shown in Fig. 1. The equilibrium cell is made of 316 stainless steel and its internal volume is about 50 cm^3 and equipped by two thermally reinforced sight glasses. The cell contents were agitated by a magnetic spin bar that was coupled with an immersion magnet placed under the cell in the bath. The bath contained about 30 L of a liquid mixture of ethylene glycol and water, which was controlled by an externally circulating refrigerator/heater. The actual operating temperature in the cell was maintained with the PID temperature controller (Jeio Tech, MC-31) with ±0.1 K accuracy and was measured by a K-type thermocouple probe with a digital thermometer (Cole-Parmer, 8535-26) of which the resolution is ±0.1 K (Every Ready Thermometer Co. Inc.). The Heise Bourdon tube pressure gauge (CMM 104957, 0-200 bar range) having the maximum error of ±0.1 bar in the full-scale range was used to measure the cell pressure in the system. For the measurement of vapor compositions at a given equilibrium condition, a sampling valve (Rheodyne, 7413) having a sampling loop of about 24.36 μL was installed and connected to a gas chromatograph (Hewlett-packard, 5890A) on-line through high-pressure metering pump (Milton Roy, 2396-31). The gas chromatograph used a thermal conductivity (TCD) and a PORAPAK-Q packed column. A vapor-sampling valve was used to perform the calibration for methane and carbon dioxide. The calibration curve for methane was fitted to first-order polynomial and carbon dioxide obtained second-order polynomial. Carbon dioxide and methane gas mixture was made by using two syringe pumps (ISCO Co. D Series). Since a syringe pump has a function of constant flow operation, the gas mixtures with known composition were introduced into the equilibrium cell. The charged gas mixture was analyzed by gas chromatograph and confirmed the desired composition.

An amount of approximately 25 ml of liquid water was initially charged into the equilibrium cell by using a metering valve. Then the equilibrium cell was charged with a mixture of carbon dioxide and methane. After the cell was pressurized to a desired pressure with a gas mixture, the system was cooled to about 5 K below the anticipated hydrate-forming temperature. Hydrate nucleation and growth was then induced and the system pressure was decreased continuously. The consumed gas mixture was recharged by using the high-pressure pump to maintain constant pressure. After the system pressure reached a steady state, the cell temperature was then very slowly elevated to dissociate the formed hydrates. The cell external heater was used to increase the system temperature at a rate of 1 to 2 K per hr. As the system approached the equilibrium temperature, the dissociation of hydrate phase caused the increase of system pressure. For maintaining the system pressure, the decomposed gas mixtures were vented through the valve connected to the cell. When the amount of minute crystals remained and system pressure was kept constant at least for 8 to 10 hr after the system temperature was stabilized, the resulting temperature and pressure were considered as three phase equilibrium conditions. When the system pressure and temperature was in equilibrium, the vapor phase was analyzed several times through the gas chromatograph. The reported equilibrium composition of the vapor phase was taken as the average values.

RESULTS AND DISCUSSION

Three-phase equilibrium conditions of hydrate, water-rich liquid and vapor (H-Lw-V) for ternary CO_2+CH_4+H_2O system were investigated at several isobaric conditions. Measured equilibrium data are tabulated in Table 2 and Table 3 and also given in Fig. 2. Fig. 2 indicates the temperature versus pressure diagrams for three phase

Table 2. Isobaric three-phase equilibrium conditions (H-L_w-V) for carbon dioxide and methane mixtures

P/bar	T/K	Vapor phase composition (CO_2 mole%)
15	272.66	40.67
	273.56	61.69
	274.36	90.41
	274.76	100.00
20	273.56	26.34
	274.36	33.75
	275.86	56.48
	276.56	79.54
	277.16	100.00
26	273.16	0.00
	275.36	18.54
	276.76	39.72
	277.96	61.95
	278.26	78.43
	279.16	100.00
35	276.16	0.00
	278.06	20.09
	279.26	42.65
	280.16	60.87
	280.76	76.17
	281.46	100.00
50	279.60	0.00
	281.46	19.71
	282.56	40.89
	283.26	59.89
	283.56	80.52

Table 3. Upper quadruple point (H-L_w-L_{CO2}-V) for carbon dioxide and methane mixtures

P/bar	T/K	Vapor phase composition (CO_2 mole %)
67.20	285.56	82.50
55.60	284.56	89.93
49.30	283.86	94.83
45.30	283.32	100.00

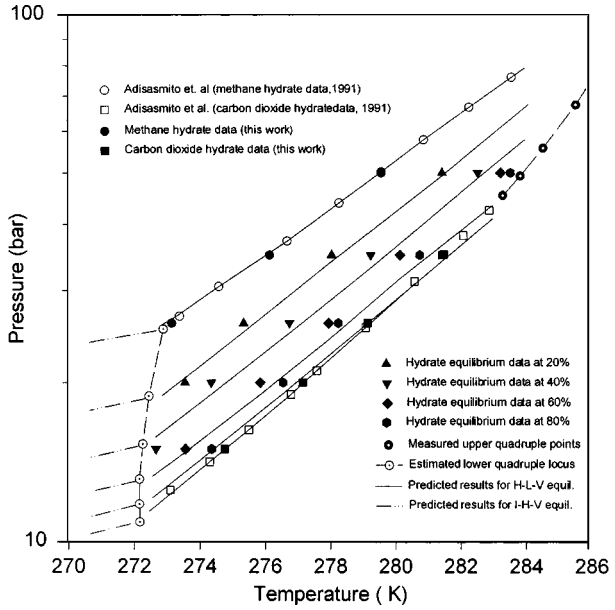

Fig. 2. Hydrate equilibrium conditions of carbon dioxide and methane mixtures.
Numbers indicate carbon dioxide mole percent in the vapor phase (water-free basis).

equilibrium conditions. It is clear from the data that the equilibrium conditions were changed between the pure carbon dioxide and methane hydrate equilibrium curves. The rate of change of equilibrium temperature was similar to that of pure methane at lower concentration than 40 mol% CO_2 concentration. But over than 60 mol% CO_2 concentration, the equilibrium conditions approached to the pure carbon dioxide equilibrium curves and were in the vicinity of that in pure carbon dioxide at 80 mol % CO_2 concentration. These phenomena can be explained by comparing the size of both guest molecules. Methane molecules enter both small and large cavities of structure I due to their small size, while carbon dioxide molecules enable them to enter only large cavities of structure I. When structure I is formed with mixture of carbon dioxide and methane, carbon dioxide molecules occupy most of the large cavities, methane molecules occupy only small cavities and small portion of large cavities. Adisasmito et al. [1992] explained a similar phenomenon. At a higher carbon dioxide concentration than 80 mol%, upper quadruple points intersect with the three-phase equilibrium curves. In this point additional CO_2-rich liquid phase (L_{CO2}) coexisted with hydrate, water-rich liquid and vapor phases. Methane does not have an upper quadruple point; the upper quadruple locus showed an endpoint. According to this study, the upper quadruple point could exist over 82.50 mol% of CO_2 concentration. In

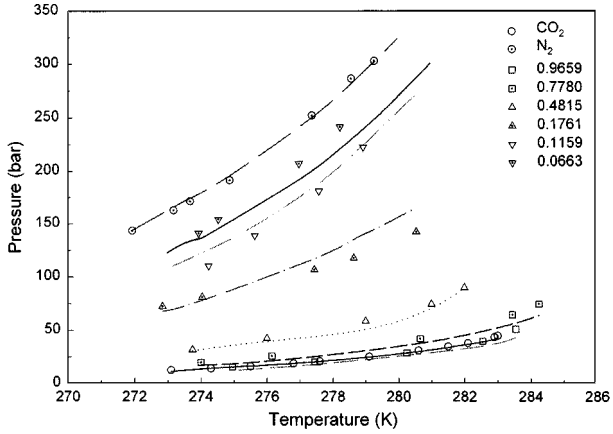

Fig. 3. Hydrate equilibrium conditions of carbon dioxide and nitrogen mixtures.
Symbols are experimental data and lines are calculation results. Number means initial loading CO_2 mole fraction. Top points of 0.9659 and 0.7780 mole fraction curve are upper quadruple points.

Table 4. Hydrate and vapor phase composition for carbon dioxide and nitrogen mixture at 274 K

Pressure (bar)	Vapor phase (CO_2)	Hydrate phase (CO_2)
13.94	1.0000	1.0000
17.69	0.8205	0.9850
23.54	0.5994	0.9517
28.35	0.5048	0.9301
35.60	0.3994	0.9001
72.35	0.2057	0.5836
112.00	0.1159	0.3426
149.28	0.0498	0.1793
179.26	0.0000	0.0000
19.53	1.0000	1.0000
26.00	0.8491	0.9782
33.77	0.5867	0.9455
52.33	0.3899	0.8867
119.80	0.1761	0.5400
155.00	0.1159	0.3526
191.74	0.0663	0.1928
240.41	0.0000	0.0000
28.01	1.0000	1.0000
36.00	0.8250	0.9765
42.33	0.6999	0.9612
50.68	0.5917	0.9432
82.75	0.3924	0.8641
149.74	0.2510	0.6400
207.53	0.1709	0.4500
266.90	0.0905	0.2217
323.08	0.0000	0.0000

addition, measured equilibrium curves are connected to the lower quadruple point where hydrate, ice (I), water-rich liquid and vapor phases coexist. In this study, the lower quadruple locus was estimated from the calculated value of two three-phase equilibrium conditions from the thermodynamic modeling results of Chun et

al. The intersection points between two equilibrium curves (hydrate-water rich liquid-vapor, hydrate-ice-vapor) are estimated as the lower quadruple point. Three-phase equilibrium data of hydrate, water-rich liquid, and vapor (H-L_w-V) for the ternary CO_2+N_2+H_2O system are presented in Fig. 3 and listed in Table 4. Measured equilibrium vapor compositions were much the same as initially introduced. However, the composition of mixed guests in hydrate and gas phase is different at equilibrium and both of them change during hydrate formation. According to various initially charged CO_2 concentrations, equilibrium conditions were drastically changed between both the pure CO_2 and N_2 hydrate H-L_w-V phase boundaries. It was clear from the data shown in Fig. 3 that the rate of change of equilibrium temperature with the mole fraction of CO_2 was high at low concentrations of CO_2, but decreased as the CO_2 content of the gas mixture increased. The results also indicated that the P-T curve of a mixed gas containing 96.59 mol% CO_2 was placed under the pure CO_2 curve. This phenomenon was considered a stabilizing effect of N_2 on mixed hydrates. CO_2 molecules fill the small and large cavities of S_I hydrate. When a small amount of N_2 was included, N_2 molecules occupied the vacant cavities that were not filled by CO_2 molecules. A similar phenomenon was observed and explained by Okui and Maeda [1997] during investigation of the CH_4+C_2H_6+H_2O system. At high CO_2 concentrations of 96.59 and 77.80 mol% upper quadruple points were also measured, where additional CO_2-rich liquid phase (L_c) coexisted with H, L_w, and V. Diamond [1994] and Bakker [1997] well explained qualitatively the phase behavior of the CO_2+N_2+H_2O system. According to their results the upper quadruple points could exist only at a CO_2 concentration greater than 85 mol%. Fig. 2 and Fig. 3 show also the predicted results of the ternary systems. All the reference properties of carbon dioxide and methane hydrate are obtained from the literature. The optimized Kihara potential parameters are presented in Table 5. Two three-phase curves, which can occur in the carbon dioxide and methane mixture system, hydrate-water rich liquid-vapor (H-L_w-V) and hydrate-ice-vapor (H-I-V), are calculated from our model and depicted in Fig. 2. The calculated values agree well with experimental hydrate-forming conditions, but especially in the H-I-V region the calculated results cannot be correlated with experimental results. The hydrate phase cannot be distinguished with ice phase at a lower temperature than the quadruple locus. The experimental work is restricted to higher temperatures than that of lower quadruple locus. Two three-phase curves coincide with one another at the lower quadruple points, and the estimated upper quadruple points agree well with experimental values. These mean that our model has a physical significance. In Fig. 2, the calculated results are in good agreement with experimental data at low concentration, but show a deviation at higher concentration than 50 mol% in high pressure region. These results might be due to the intrinsic uncertainty of the modified UNIFAC model. The calculated results are also in good agreement with our experimental data in Fig. 3. Deviations at low CO_2 concentrations were rather larger than that of high CO_2 concentrations and calculated values were underestimated in general. Our model well explained even the stabilizing effect of N_2 on mixed hydrates. Calculated equilibrium pressures for 96.59 mol% CO_2 gas mixture were below the pure CO_2 calculated pressures. CO_2 forms S_I hydrate, and N_2 forms S_{II} hydrate. If CO_2-rich gas mixture were introduced, obtained hydrate would be S_I and vice versa. Figs. 2-4 show that there is no severe P-T slope change from hydrate structure transformation. But, the well-known Sloan's CSMHYD which produces 15 mol% of CO_2 is the borderline of two kinds of hydrate structures. In our model calculation, 12 mol% of CO_2 mixture was obtained.

Table 5. Optimized Kihara potential parameters for carbon dioxide and nitrogen

	a (Å)	σ (Å)	ε/k (Å)
CO_2	0.7200	2.8870	188.60
CH_4	0.3000	3.2408	153.20
N_2	0.3526	3.0298	125.07

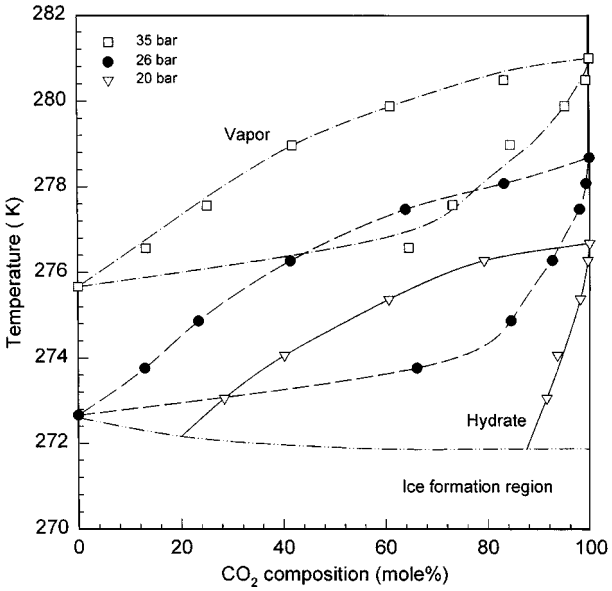

Fig. 4. Temperature-composition diagram of carbon dioxide and methane mixtures.

Table 6. Hydrate and vapor compositions for carbon dioxide and methane mixtures at isobaric conditions

P/bar	T/K	Vapor phase composition	Hydrate phase composition
20	273.06	28.44	91.51
	274.06	40.25	93.63
	275.36	60.76	98.15
	276.26	79.44	99.65
26	273.76	12.93	66.18
	274.86	23.44	84.68
	276.26	41.46	92.72
	277.46	64.11	98.08
	278.06	83.39	99.35
35	276.56	13 .25	64.72
	277.56	25.23	73.34
	278.96	41.91	88.99
	279.86	61.13	95.23
	280.46	83.44	99.30

Fig. 4 shows the hydrate compositions in equilibrium with the vapor phase at constant pressure and the experimental results are given in Table 6. It is clear from the data that carbon dioxide is more included into the hydrate phase dominantly than methane in a wide range of composition. This is because the composition of the hydrate phase is determined mainly by the equilibrium vapor phase composition and the system pressure. The composition of carbon dioxide in the hydrate phase increases with increasing the carbon dioxide composition in the vapor phase and decreasing the system pressure. When the vapor composition is higher than 40 carbon dioxide mole%, the concentration of carbon dioxide in the hydrate phase is higher than 90 mol%. At 40 mol% CO_2 mixture, the corresponding equilibrium hydrate phase carbon dioxide compositions were about 93.63, 92.72 and 88.99 mol% at 20, 26, 35 bar, respectively. This means that lower pressure has better carbon dioxide selectivity. It is expected that carbon dioxide can create a long-lived hydrate lake on the ocean floor by injection into the natural gas hydrate deposits. Injected carbon dioxide stream results in the dissociation of natural gas hydrate, and subsequent growth of carbon dioxide hydrate will occur. Therefore, the formed hydrate phase is occupied mainly by carbon dioxide and the dissociated natural gas can be exploited simultaneously.

From Fig. 3, we selected 274, 277, and 280 K as isotherm lines and measured the equilibrium vapor and hydrate phase compositions. Results are listed in Table 7 and illustrated in Fig. 5. Measurement of hydrate phase composition is a very difficult job although some experimental data for limited systems were published [van der Waals and Platteeuw, 1959; Thakore and Holder, 1987]. Most of them were under low temperature and medium pressure ranges. Recently, some researchers have been trying to measure the equilibrium hydrate composition with Raman spectroscopy, which can measure the three-phase (H-L_w-V) equilibrium conditions. But it is very expensive instrument. Therefore, in this study we used a relatively cheap and easy method, gas chromatography. The whole of the experimental data listed in Table 7 was under two-phase (H-V) region, but experimental pressure was very close to three-phase conditions. As seen in Fig. 5, the isothermal P-x diagram is similar to the VLE figure. Lines represent the calculated results. Our model calculation shows good agreement with the equilibrium vapor and hydrate phase composition data. The equilibrium hydrate composition of CO_2 increased as its vapor phase composition increased. Temperature increase resulted in higher equilibrium pressure. At 15 mol% CO_2 mixture, the corresponding equilibrium hydrate phase CO_2 compositions were about 56, 47, and 36 mol% at 274, 277, and 280 K, respectively. This means that lower temperature has better CO_2 selectivity. In addition, corresponding equilibrium pressure was lowered at lower temperature. At 274 K, if 17 mol% CO_2 mixture were introduced, the expected hydrate would be 58 mol% CO_2. If this hydrate were dissociated, the same composition gas mixture would be obtained. When this gas mixture was introduced again, the corresponding equilibrium hydrate phase would be over 95 mol% of CO_2. This is familiar to the distillation process. From this isothermal P-x diagram, selective gas separation method can be organized.

Table 7. Hydrate and vapor phase composition for carbon dioxide and nitrogen mixtures at 274 K

Pressure (bar)	Vapor phase (CO_2)	Hydrate phase (CO_2)
13.94	1.0000	1.0000
17.69	0.8205	0.9850
23.54	0.5994	0.9517
28.35	0.5048	0.9301
35.60	0.3994	0.9001
72.35	0.2057	0.5836
112.00	0.1159	0.3426
149.28	0.0498	0.1793
179.26	0.0000	0.0000
19.53	1.0000	1.0000
26.00	0.8491	0.9782
33.77	0.5867	0.9455
52.33	0.3899	0.8867
119.80	0.1761	0.5400
155.00	0.1159	0.3526
191.74	0.0663	0.1928
240.41	0.0000	0.0000
28.01	1.0000	1.0000
36.00	0.8250	0.9765
42.33	0.6999	0.9612
50.68	0.5917	0.9432
82.75	0.3924	0.8641
149.74	0.2510	0.6400
207.53	0.1709	0.4500
266.90	0.0905	0.2217
323.08	0.0000	0.0000

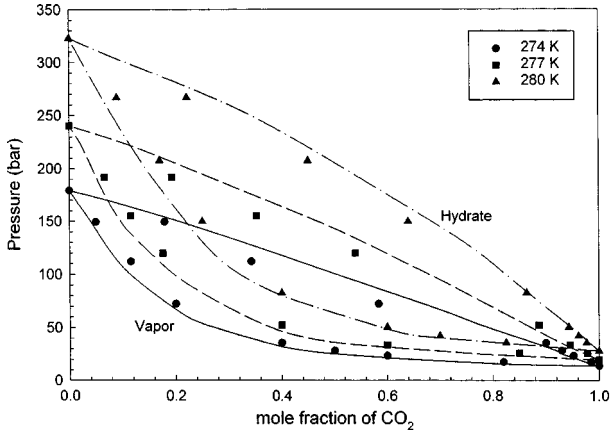

Fig. 5. Pressure-composition diagram of the carbon dioxide and nitrogen mixtures.

CONCLUSIONS

Three-phase (H-L_w-V) equilibrium dissociation conditions for mixed hydrates of CO_2-CH_4 and CO_2-N_2 were measured experimentally. The quadruple locus, where the four phases (H-L_w-L_{CO2}-V) coexist, was also particularly determined. The equilibrium data were predicted by the SRK-EOS with MHV mixing rule incorporated with the modified UNIFAC method. The only estimated parameters are two Kihara energy and size parameters, ε and σ, obtained by fitting all experimental data in the hydrate-forming region. Conclusively, the equilibrium calculation model is thermody-

namically reasonable and offers the accurate prediction of thermodynamic properties to the process using hydrate formation.

ACKNOWLEDGMENT

This work was supported by grant No. 98-0502-04-01-3 from the Basic Research program of the KOSEF and also partially by the Brain Korea 21 Project.

NOMENCLATURE

a : parameter in the equations of state or radius of the spherical core
a_w : activity of water
a_{mn} : group interaction parameter for the interaction between groups m and n
b : parameter in the equations of state
C_{m_j} : Langmuir constants
f : fugacity of the gas [bar]
f_i^{MT} : fugacity of host component in the empty clathrate lattice
$f_i^{L^o}$: fugacity of pure host component
g : Gibbs free energy
Δg : free energy change per unit volume of product [J/m^3]
$\Delta h_i^{MT-L^o}$: differences in enthalpy between empty hydrate lattice and liquid water
K : rate constant of hydrate formation kinetics
n : number of moles
n_w : number of water molecules per gas molecule
P : pressure [bar]
Q_k : surface area parameter for group k
q_1, q_2 : mixing rule constants in modified Huron-Vidal mixing rule
R : universal gas constant
R_k : volume parameter for group k
r : radial distance from the center of the cavity [Å]
T : temperature [K]
t : time [s]
V : volume [m^3]
ν : molar volume
ν_o : feed gas velocity [m/s]
$\Delta\nu_i^{MT-L^o}$: differences in volume between empty hydrate lattice and liquid water
ν_m : molar volume of the hydrate [m^3/mol]
ν_w : molar volume of water [m^3/mol]
x : liquid phase mole fraction
y : gas phase mole fraction
z : coordination number

Greek Letters

α : equation of state parameter, α=a/bRT or hydrate conversion parameter
$\Gamma_k^{(i)}$: the residual activity coefficient of group k in a reference solution containing only molecules of type i
γ : activity coefficient
φ : fugacity coefficient
ν_m : number of cavities of type m per host molecule
ν_{ki} : number of groups of type k in molecule i
$\omega(r)$: spherically symmetrical cell potential
σ : distance between the cores at zero potential energy
ε : depth of the intermolecular potential well
τ : retention time
$\Delta\mu_i^{MT-C}$: difference between the chemical potentials of host component in the empty clathrate lattice and pure host component at T and P
$\Delta\mu_i^{o}$: difference between the chemical potentials of the empty clathrate lattice and the pure host component at T^o and zero absolute pressure

Superscripts

E : excess property
C : combinatorial contribution
o : standard state, 273.15 K and 1 bar
R : residual contribution

Subscripts

i, j, k : molecular species
m : mixture
∞ : infinite pressure state
c : critical state
eq : three-phase equilibrium condition
exp : experimental condition
g : gas phase
L : liquid phase
o : time at start
t : time at t
w : water

REFERENCES

Adisasmito, S., Frank III, R. J. and Sloan, Jr., E. D., "Hydrates of Carbon Dioxide and Methane Mixtures," *J. Chem. Eng. Data*, **36**, 68 (1991).

Adisasmito, S. and Sloan, Jr., E. D., "Hydrates of Hydrocarbon Gases Containing Carbon Dioxide," *J. Chem. Eng. Data*, **37**, 343 (1992).

Bakker, R. J., "Clathrates: Computer Programs to Calculate Fluid Inclusion V-X Properties Using Clathrate Melting Temperatures," *Computers & Geosciences*, **23**, 1 (1997).

Berecz, E. and Balla-Achs, M., "Gas Hydrates," Elsevier, Amsterdam (1983).

Diamond, L. W., "Salinity of Multivolatile Fluid Inclusions Determined from Clathrate Hydrate Stability," *Geochimica et Cosmochimica Acta*, **58**, 19 (1994).

Englezos, P., "Clathrate Hydrates," *Ind. Eng. Chem. Res.*, **32**, 1251 (1993).

Holder, G. D., Corbin, G. and Papadopoulos, K. D. "Thermodynamic and Molecular Properties of Gas Hydrates from Mixtures Containing Methane, Argon, and Krypton," *Ind. Eng. Chem. Fundam.*, **19**, 282 (1980).

Holder, G. D., Zetts, S. P. and Pradhan, N., "Phase Behavior in Systems Containing Clathrate Hydrates," *Reviews in Chemical Enginnering*, **5**, 2 (1988).

Huron, M. J. and Vidal, J., "New Mixing Rules in Simple Equations of State for Representing Vapor-Liquid Equilibria of Strongly Non-

Ideal Mixtures," *Fluid Phase Equilibria*, **3**, 255 (1979).
Jhaveri, J. and Robinson, D. B., "Hydrates in the Methane-Nitrogen System," *Can. J. Chem. Eng.*, **April**, 75 (1965).
Makogon, Y. F., "Hydrates of Hydrocarbons," PennWell Books, Tulsa (1997).
McKoy, V. and Sinanoglu, O., "Theory of Dissociation Pressures of Some Gas Hydrates," *J. Chem. Phys*., **38**, 2946 (1963).
Okui, T. and Maeda, Y., "Hydrates with Multiple Guests," Int'*l* Workshop on Gas Hydrates Studies, The 2nd Joint Japan-Canada Workshop, Tsukuba, Japan, 98 (1997).
Parrish, W. R. and Prausnitz, J. M., "Dissociation Pressures of Gas Hydrates Formed by Gas Mixtures," *Ind. Eng. Chem. Process Des. Dev.*, **11**, 267 (1972).
Sloan, E. D. Jr., "Clathrate Hydrates of Natural Gases," Marcel Dekker, New York (1990).
Soave, G., "Equilibrium Constants from a Modified Redlich-Kwong Equation of State," *Chem. Eng. Science*, **27**, 1197 (1972).
Unruh, C. H. and Katz, D. L., *Pet. Trans*. AIME (1949) 83-86.
van der Waals, J. H. and Platteeuw, J. C., "Clathrate Solutions," *Adv. Chem. Phys*., **2**, 1 (1959).